Theor Appl Climatol
DOI 10.1007/s00704-017-2166-x

ORIGINAL PAPER

Variability of cold season surface air temperature over northeastern China and its linkage with large-scale atmospheric circulations

Yuanhuang Zhuang[1,2] · **Jingyong Zhang**[1,2] · **Lin Wang**[1]

Received: 11 October 2016 / Accepted: 8 May 2017

Abstract Cold temperature anomalies and extremes have profound effects on the society, the economy, and the environment of northeastern China (NEC). In this study, we define the cold season as the months from October to April, and investigate the variability of cold season surface air temperature (CSAT) over NEC and its relationships with large-scale atmospheric circulation patterns for the period 1981–2014. The empirical orthogonal function (EOF) analysis shows that the first EOF mode of the CSAT over NEC is characterized by a homogeneous structure that describes 92.2% of the total variance. The regionally averaged CSAT over NEC is closely linked with the Arctic Oscillation (r = 0.62, 99% confidence level) and also has a statistically significant relation with the Polar/Eurasian pattern in the cold season. The positive phases of the Arctic Oscillation and the Polar/Eurasian pattern tend to result in a positive geopotential height anomaly over NEC and a weakened East Asian winter monsoon, which subsequently increase the CSAT over NEC by enhancing the downward solar radiation, strengthening the subsidence warming and warm air advection. Conversely, the negative phases of these two climate indices result in opposite regional atmospheric circulation anomalies and decrease the CSAT over NEC.

✉ Yuanhuang Zhuang
zhuangyuanhuang14@mails.ucas.ac.cn

[1] Center for Monsoon System Research, Institute of Atmospheric Physics, Chinese Academy of Sciences, Beijing 100029, China

[2] University of Chinese Academy of Sciences, Beijing 100049, China

1 Introduction

Northeastern China (NEC), located in the east of Eurasia, is featured with the coldest climate in China. The regional mean surface air temperature (SAT) in the boreal winter can be as low as −15 °C. Below-normal temperature anomalies and extreme cold events over NEC cause large losses to both the economy and the society. For example, in December 2009, frequent severe snow storms resulted in direct economic losses of up to 7 billion yuan (Wang and Chen 2010). An exceptionally heavy snowfall that occurred in NEC in April 2010 causes severe travel difficulties and increases traffic accidents. On the other hand, the cold climate also benefits NEC with events such as the Harbin International Ice Festival and the winter fishing festival in Chagan Lake, Jilin Province, which provide opportunities for the tourism sector.

The variability in the wintertime SAT over NEC is strongly influenced by the East Asian winter monsoon (EAWM) and shows substantial inter-annual and inter-decadal variabilities (Kang et al. 2006, 2009; Huang et al. 2012; Alessio et al. 2014; Ding et al. 2014; Hu et al. 2015). When the EAWM is active and strong, the Siberian high (SH) often extends eastward, leading to frequent outbreaks of cold air, i.e., cold waves (Ding and Krishnamurti 1987). As a result, the temperature drops sharply and severeweather is observed in NEC (Zhang et al. 1997; Li and Yang 2010; Wang and Chen 2010; Wang et al. 2011). Large-scale atmospheric circulation patterns can influence the EAWM and winter SAT over NEC (Wang and Lu 2017). For example, the positive (negative) phase of the Northern Hemisphere Annular Mode/Arctic Oscillation (AO) can weaken (strengthen) the EAWM and lead to warm (cold) winter over NEC (Gong et al. 2001; Wu and Wang 2002; Li and Wang 2003a; Chen et al. 2005; Hu and Liu 2005). The North Atlantic Oscillation (NAO) (Wu and Huang 1999; Gong 2000; Li and Wang 2003b; Hong et al. 2008), the Southern

Published online: 26 May 2017

Annular Mode (Wu et al. 2009), and the event of the stratospheric processes (Chen et al. 2013a; Lan and Chen 2013; Lu and Ding 2015) can also affect the winter SAT in NEC.

A year is traditionally divided into four seasons. Winter is usually defined as December through to February in many studies. However, this conventional definition may not be suitable for the NEC climate studies because the cold period in this region is much longer than 3 months. Previous studies about the division of four seasons over China show that the start dates of four seasons over NEC is about in April, June, late August, and October, respectively (Zhang 1934; Zhang and Lin 1985; Yu et al. 2010). This implies that the transitional season is very short, while the winter can persist up to around 7 months over NEC. In this study, we revisit the definition of winter in NEC and take the cold season as the months from October to April. Based on this definition, we investigate the variability of the cold season SAT (CSAT) over NEC and its relationships with large-scale atmospheric circulation patterns.

Section 2 introduces the datasets and methods used. Section 3 justifies the new definition of the cold season for NEC, and Sect. 4 investigates the first two empirical orthogonal function (EOF) modes of the variability of the CSAT over NEC. The relationships between the CSAT in NEC and the large-scale atmospheric circulation patterns over the Northern Hemisphere are examined in Sect. 5. Section 6 explains the linkage between the cold season large-scale climate indices and the CSAT over NEC, and main conclusions are drawn in Sect. 7.

2 Data and methods

We use the daily mean SAT data from the European Centre for Medium-Range Weather Forecasts Interim Reanalysis (ERA-Interim) dataset (Dee et al. 2011) and the gridded SAT dataset from the Climatic Research Unit Version 4.00 (CRU TS4.00) dataset. The latter is based on monthly observations at meteorological stations across the world's land areas for the period 1901–2014, with a spatial resolution of 0.5 × 0.5° (Harris et al. 2014). Table 1 lists the names and sources of large-scale climate indices used in this study, which include the AO, the NAO, the NINO3.4, the Polar/Eurasia pattern (POL), Pacific Decadal Oscillation (PDO), Pacific/North American (PNA), and Atlantic Multidecadal Oscillation (AMO) indices. To examine the possible physical reasons for CSAT variability over NEC and large-scale atmospheric circulation patterns over the Northern Hemisphere, we use the monthly mean ERA-Interim data for atmospheric circulation patterns' variables, including sea-level pressure (SLP), geopotential height, and the wind vector on a 0.5° × 0.5° grid. The shortwave and longwave radiations and sensible and latent heat fluxes are from the National Centers for Environment Prediction-US Department of Energy (NCEP-DOE) AMIP-II reanalysis (Kanamitsu et al. 2002) that spans from 1979 to the present.

The period considered in this study is 1981–2014. To reveal the dominant patterns of the CSAT variability, the EOF analysis (von Storch and Zwiers 1999) is used to extract the leading modes. The EOF analysis, without a fixed function form and fast speed of convergence, is commonly used to examine the spatiotemporal characteristics of climate variables. The EOF technique splits the temporal variance of climate variables into several orthogonal spatial patterns called empirical eigenvectors to explain the variation in variance of climate variables as far as possible through a linear combination of climate variables.

When the pentad is concerned, we use the traditional Chinese definition of pentad, which has 72 pentads throughout the year. In this definition, each month is divided into six pentads and the first five pentads are 5 days. The last pentad is defined as from the 26th day to the last day of the month. Therefore, in the months that have 31 (30) days, the last pentad has 6 (5) days. In February of the leap (non-leap) years, the last pentad has 4 (3) days.

Table 1 Climate indices used in this study, time period, and their source

Name	Explanation	Period	Data source
AO	Arctic Oscillation	1950–2015	http://www.cpc.ncep.noaa.gov/products/precip/CWlink/daily_ao_index/ao.shtml
NAO	North Atlantic Oscillation	1950–2015	http://www.cpc.ncep.noaa.gov/data/teledoc/nao.shtml
NINO3.4	NINO index	1948–2015	http://www.esrl.noaa.gov/psd/data/correlation/nina34.data
POL	Polar/Eurasia	1950–2015	http://www.cpc.ncep.noaa.gov/data/teledoc/poleur.shtml
PDO	Pacific Decadal Oscillation	1948–2015	http://research.jisao.ishington.edu/pdo/PDO.latest
PNA	Pacific North American	1950–2015	http://www.cpc.ncep.noaa.gov/data/teledoc/pna.shtml
AMO	Atlantic Multidecadal Oscillation	1948–2015	http://www.esrl.noaa.gov/psd/data/correlation/amon.us.data

The relationships between the CSAT variability over NEC and the large-scale atmospheric circulation patterns are examined by correlation and regression analyses. Two-sided Student's *t* test is used to judge the confidence levels of the correlation and regression.

3 Definition of the cold season in northeastern China

In operational practices, the China Meteorological Administration defines the beginning of winter when the pentad averaged SAT is lower than 10 °C. According to this standard, the winter season of NEC is much longer than 3 months (Zhang 1934; Zhang and Lin 1985; Yu et al. 2010). Figure 1 shows that the pentad average SAT values averaged over 1981–2014 are all lower than 10 °C from October through to April. We also calculate the 1981–2014 monthly mean SAT values for NEC and find that they are all lower than 5 °C from October through to April (Fig. 2). These results suggest that the cold season can be defined as October through April in NEC.

To further justify the suitability of this definition, we compare the 850 hPa wind field in each month with that in winter and summer. Strong northwesterly winds are observed over NEC in winter (Fig. 3a), and weaker southwesterly winds are observed in summer (Fig. 3b). When each month is examined, it reveals that the wind fields in March, April, October, and November quite resemble that in winter (Fig. 3c–h). We further calculate the spatial correlation between the winter mean wind fields with the monthly wind field. Here the spatial

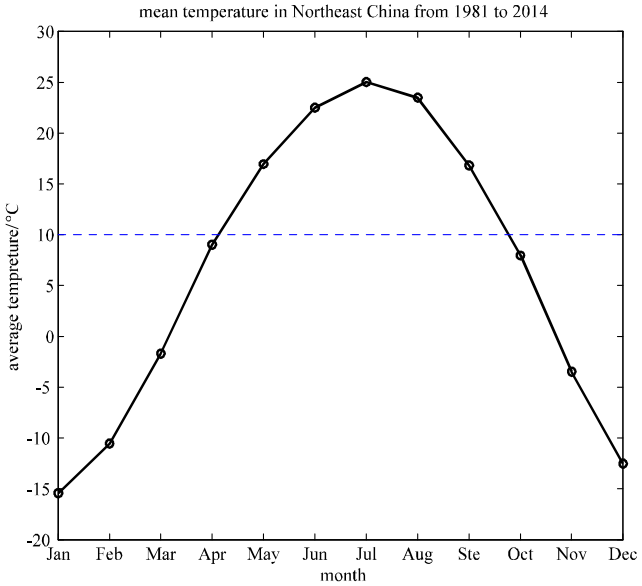

Fig. 2 The time series of the monthly mean area-averaged surface air temperature in NEC from January to December for 1981–2014 (unit: °C; the *blue dashed line* indicated 10 °C)

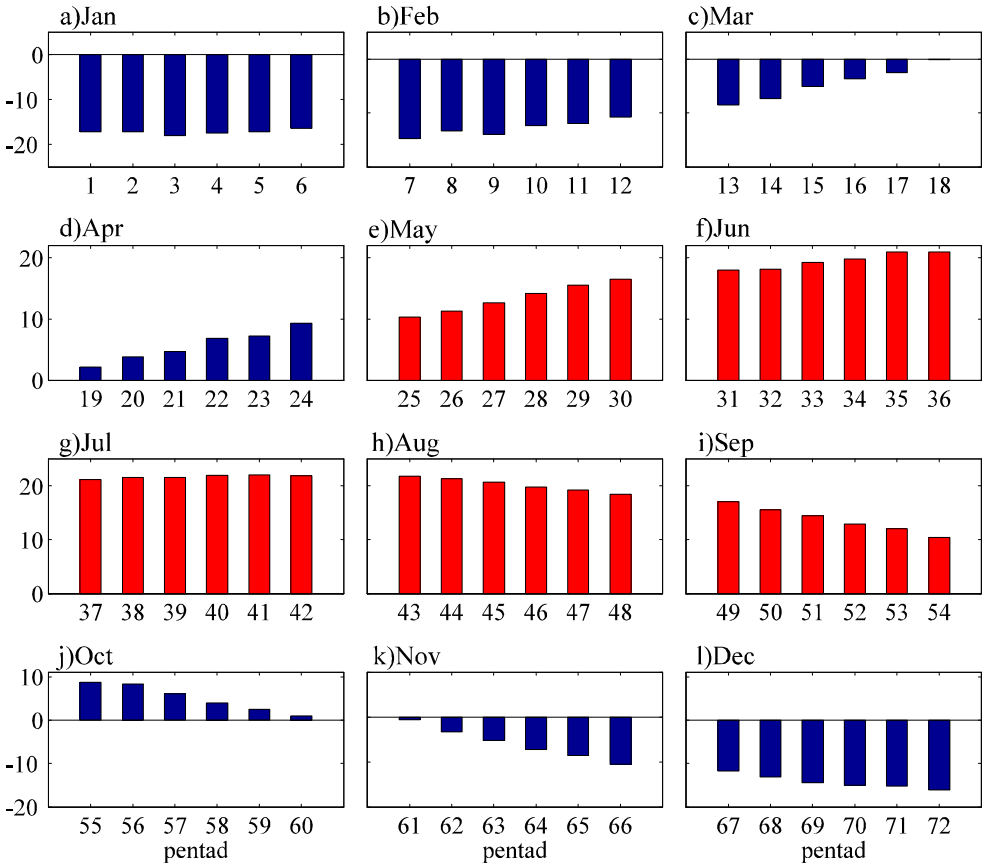

Fig. 1 Pentad average temperature over NEC from pentad 1 to pentad 72 during 1981–2014 (unit: °C). **a**–**l** January–December; *blue*: below 10 °C; *red*: more than 10 °C

correlation coefficient is calculated with the combination of zonal and meridional wind components over the region extending from 38° to 60° N and from 100° to 140° E. It reveals that the correlation coefficients from October to April all exceed 0.6, significant at the 99.9% confidence level (Fig. 4). In May and September, the correlation coefficients are also significantly at the 99% confidence level (Fig. 4), probably because of the large contribution of the zonal westerly wind as shown in Fig. 3d, g. Combining the results of temperature and wind field, we, therefore, define the cold season as the months from October to April in NEC.

Based on this new definition, there are a total of 33 cold seasons in our study during 1981–2014. The cold season of 1981 refers to October 1981 to April 1982. The following sections will discuss the variability in the CSAT over NEC and its linkage with large-scale atmospheric circulation patterns.

4 Characteristics of the spatiotemporal variability in the CSAT over NEC

An EOF analysis was performed on the CSAT over NEC, and the first two EOFs are shown in Fig. 5. The first EOF mode explains 92.2% of the total variance and shows a monopole structure with the highest loadings over the north of eastern Inner Mongolia and the junction of Jilin and Heilongjiang provinces (Fig. 5a). This suggests a homogeneous temperature anomaly over NEC. The corresponding first principal component (PC1) is highly correlated with the area-averaged

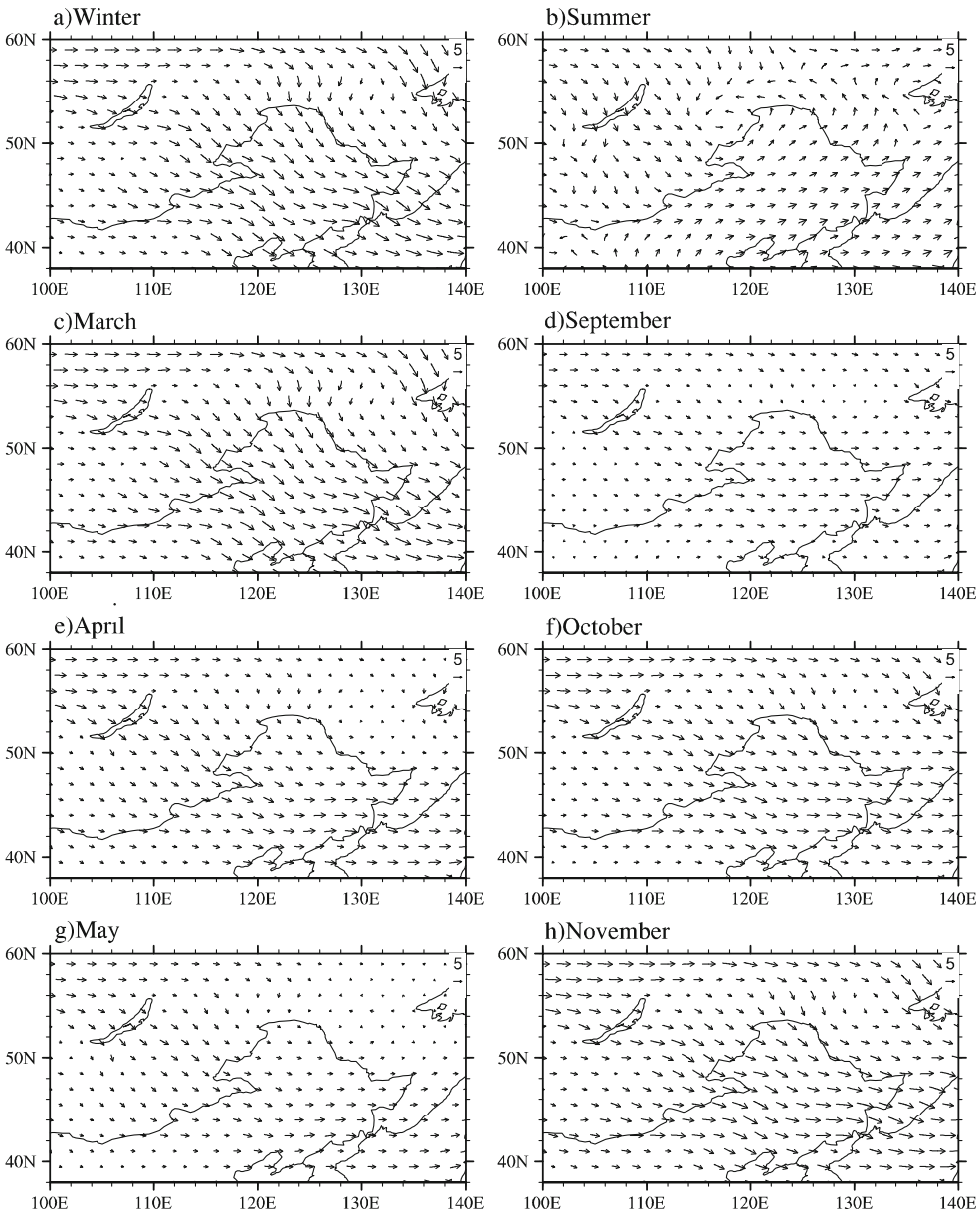

Fig. 3 The climatological wind field. **a** Winter. **b** Summer. **c** March. **d** September. **e** April. **f** October. **g** May. **h** November at 850 hPa ($m \cdot s^{-1}$; vectors; scale at *upper-right corner*)

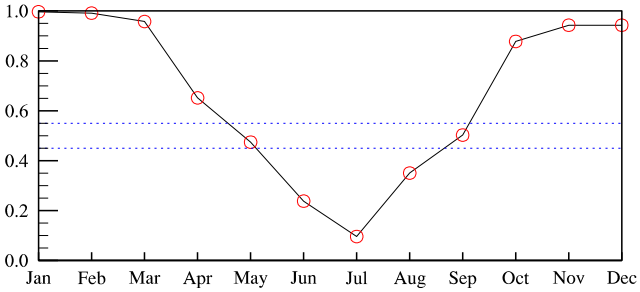

Fig. 4 The correlation coefficient of the wind field between the winter and monthly from January to December at 850 hPa (*two dashed lines* denote the 99 and 99.9% confidence levels based on a two-sided Student's *t* test, respectively)

CSAT over NEC ($r = 0.9$, 99.9% confidence level), indicating that PC1 is a good reflection of the whole regional area-averaged CSAT anomalies (Fig. 5b). Further analysis shows that PC1 is significantly correlated with the cold season SH and the East Asian winter monsoon index ($r = -0.45$/ $r = -0.47$, after removing their long-term linear trends, 99% confidence level). Here the intensity of SH is defined as the regionally averaged SLP over 40°–60° N, 50°–120° E in cold season, and the East Asian winter monsoon index (EAWMI) follows Jhun and Lee (2004). This suggests the CSAT over NEC is mainly affected by the East Asian winter monsoon system. As will be shown later, the cold season geopotential height anomalies, corresponding to PC1, show a monopole structure with the positive center being located over the East of Lake Baikal. This may explain why the variance contributed by the first EOF mode is so high.

The second EOF pattern of the CSAT (Fig. 5c), which describes 4.5% of the total variance, has a dipole-like structure with negative anomaly loadings over the northern part of NEC and positive anomaly loadings over the southern part of NEC. The zero line is oriented northwest–southeast, implying an opposite CSAT anomaly between the northern and southern areas of NEC. The corresponding PC2 (Fig. 5d) shows a pronounced inter-annual variability.

The CSAT anomaly over NEC exhibits a pronounced inter-annual variability (Fig. 5b). The warmest cold seasons over NEC, in terms of the CSAT, occur after 1985 and are recorded for 2001 (1.9 °C higher), 1988 (1.3 °C higher), and 2013 (1.3 °C higher). The coldest cold seasons over NEC occur after 2000 and are recorded for 2012 (2.1 °C lower), 2009 (2 °C lower), and 2000 (1.6 °C lower), respectively. The strong inter-annual variability, under the background of global climate change, shows why the CSAT over NEC does not

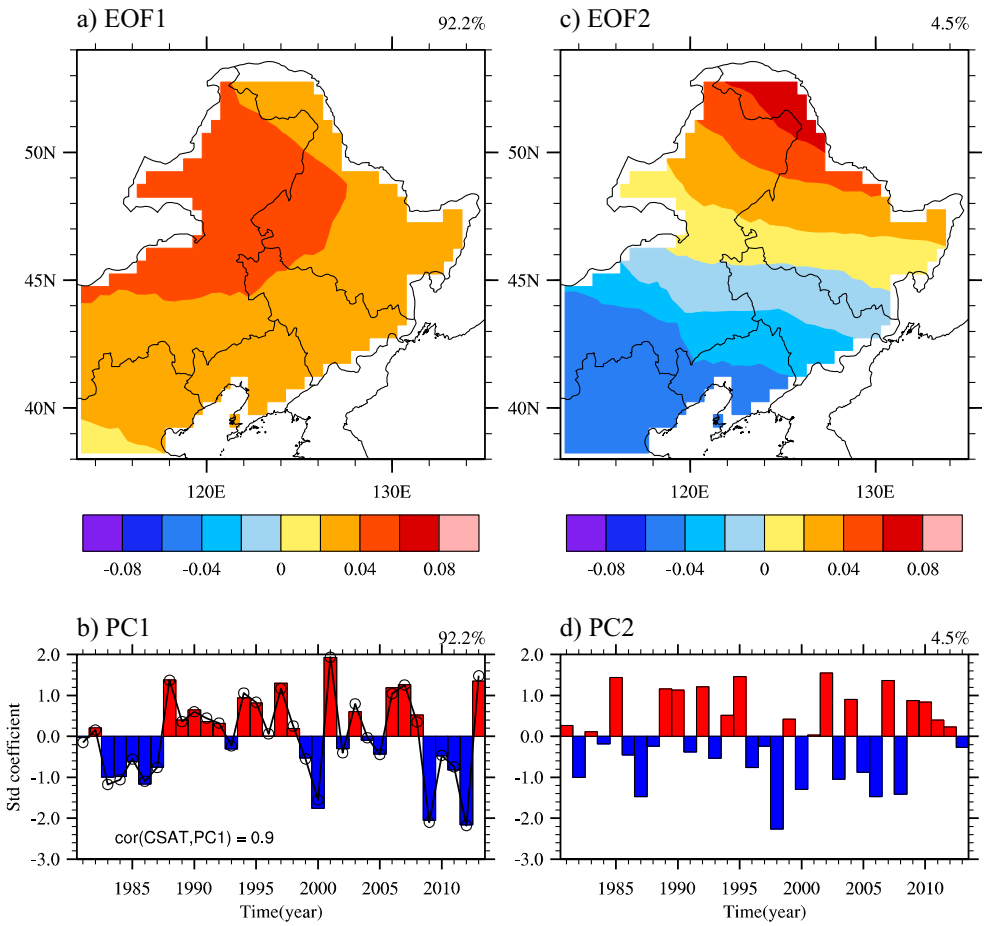

Fig. 5 Spatial patterns of the first two leading EOF modes of CSAT over NEC and the corresponding normalized principal competent (PC) time series. **a** The first EOF mode. **b** Time series of the first EOF mode (PC1). **c** The second EOF mode. **d** Time series of the second EOF mode (PC2). The *solid line with an asterisk* in **b** denotes the standardized series of CSAT

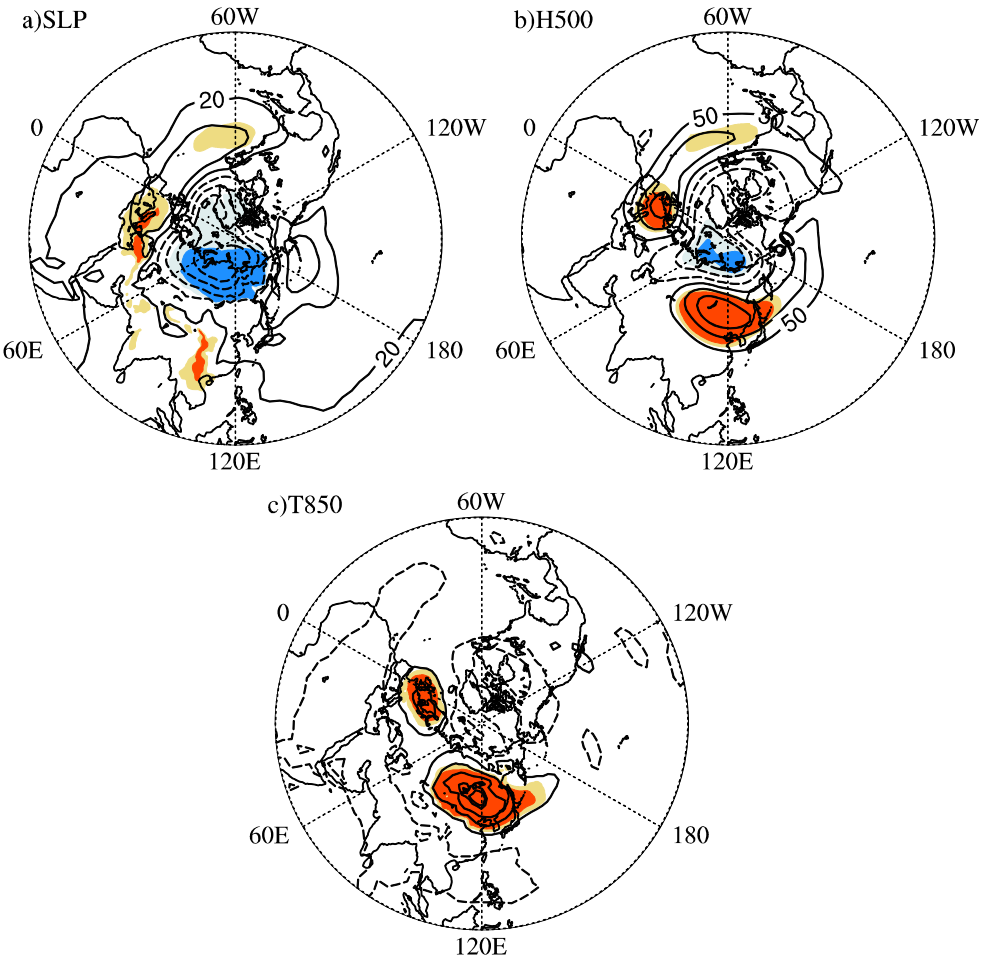

Fig. 6 Regression maps for **a** sea-level pressure, **b** 500 hPa geopotential height, and **c** 850 hPa CSAT over Northern Hemisphere based on the CSAT over NEC from 1981 to 2014 (*light and dark shadings* indicate the 99 and 99.9% confidence levels based on a two-sided Student's *t* test, respectively). The contour interval is 80 hPa, 100 gpm, and 0.5 °C in **a**, **b**, and **c** respectively. The *dashed line* indicates a negative value, and the *solid line* shows the positive value

obviously increase during the period 1981–2014. In addition, the CSAT over NEC also has an obvious inter-decadal variation with a warming period 1987 to 2007 and cooling periods 1981 to 1986 and 2008 to 2014. This is generally consistent with the decadal variability of the East Asian winter monsoon (Wang et al. 2009; Wang and Chen 2014; Ding et al. 2014), and it is also likely to be related to the global warming or arctic amplification (Graversen et al. 2012; Ding et al. 2014).

5 Large-scale atmospheric circulation patterns associated with the CSAT anomaly

To analyze the characteristics of the large-scale atmospheric circulation patterns associated with the CSAT anomaly, we construct regression maps for SLP, the 500 hPa geopotential height anomaly (H500), and 850 hPa the temperature anomaly (T850) for the cold season based on the time series of area-averaged CSAT over NEC.

Figure 6 shows the characteristics of atmospheric circulation patterns associated with the CSAT anomaly over NEC for 1981–2014. During the cold season, the negative SLP anomaly extends from the polar region to Siberia over the Eurasian

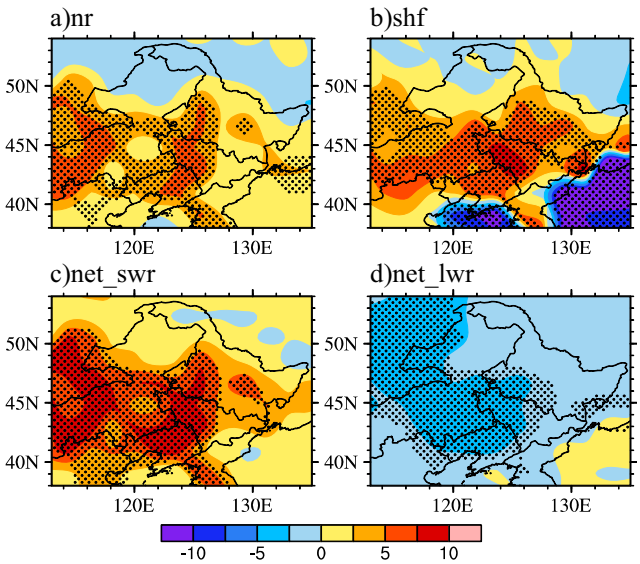

Fig. 7 Regression maps for surface **a** net radiation, **b** sensible heat flux, **c** net shortwave radiation, and **d** net longwave radiation based on the CSAT over NEC from 1981 to 2014 (*dots* indicate regions where the regression correlations are exceeding the 95% confidence level). Net radiation (net shortwave radiation plus net longwave radiation). Net shortwave radiation (net downward shortwave radiation minus net upward shortwave radiation), and net longwave radiation (net downward longwave radiation minus net upward longwave radiation)

continent and the positive SLP anomaly is located in the North Atlantic (Fig. 6a). NEC is dominated by an anomalous anticyclonic circulation. The H500 increases over the areas south of 50° N and decreases over the areas north of 50° N over East Asia (Fig. 6b). The strong positive anomaly over NEC weakens the East Asian major trough and strengthens the high ridge in the west of Lake Baikal. Therefore, the East Asian region's meridional circulation is weaker than the zonal westerly circulation. This suggests that when the CSAT over NEC is warmer than normal, the Siberian high and the Aleutian low weaken at SLP, and this anticyclonic circulation strengthens and the East Asian major trough weakens at H500. The configuration of this circulation is conducive to warm CSAT anomalies over large area of northeastern Siberia (Fig. 6c).

To investigate how the warm anomalies are induced, we examined the effects of advection and radiation. Figure 7 shows the CSAT-related anomalies of cold season surface net radiation (NR), sensible heat flux (SHF), shortwave radiation (SWR), and longwave radiation (LWR) by regression on the CSAT over NEC from 1981 to 2014. Positive net radiation denotes downward, indicating heating effect on the ground surface. A significant NR increase is observed throughout most NEC (Fig. 7a), which is dominated by downward SWR (Fig. 7c). This is likely caused by the clear sky, which is controlled by the anomalous anticyclone (Fig. 6b). Although the LWR tends to cool the ground (Fig. 7d), its effect is weaker than the SWR (Fig. 7c). This result suggests that the ground surface receives more heat from the downward solar radiation to warm the surface (Fig. 7a). When the ground is heated and warmer than the surface air, it will lead to upward sensible heat flux to warm the air (Fig. 7b), thereby contributing constructively to the warmer CSAT (Fig. 6c).

Figure 8 shows that the advection effect generally favors the observed temperature change. A further inspection suggests that the advection of anomalous temperature by basic wind is constructive (Fig. 8b), while the advection of basic temperature by anomalous winds is destructive (Fig. 8e). To understand this process, Fig. 9 shows the climatological mean

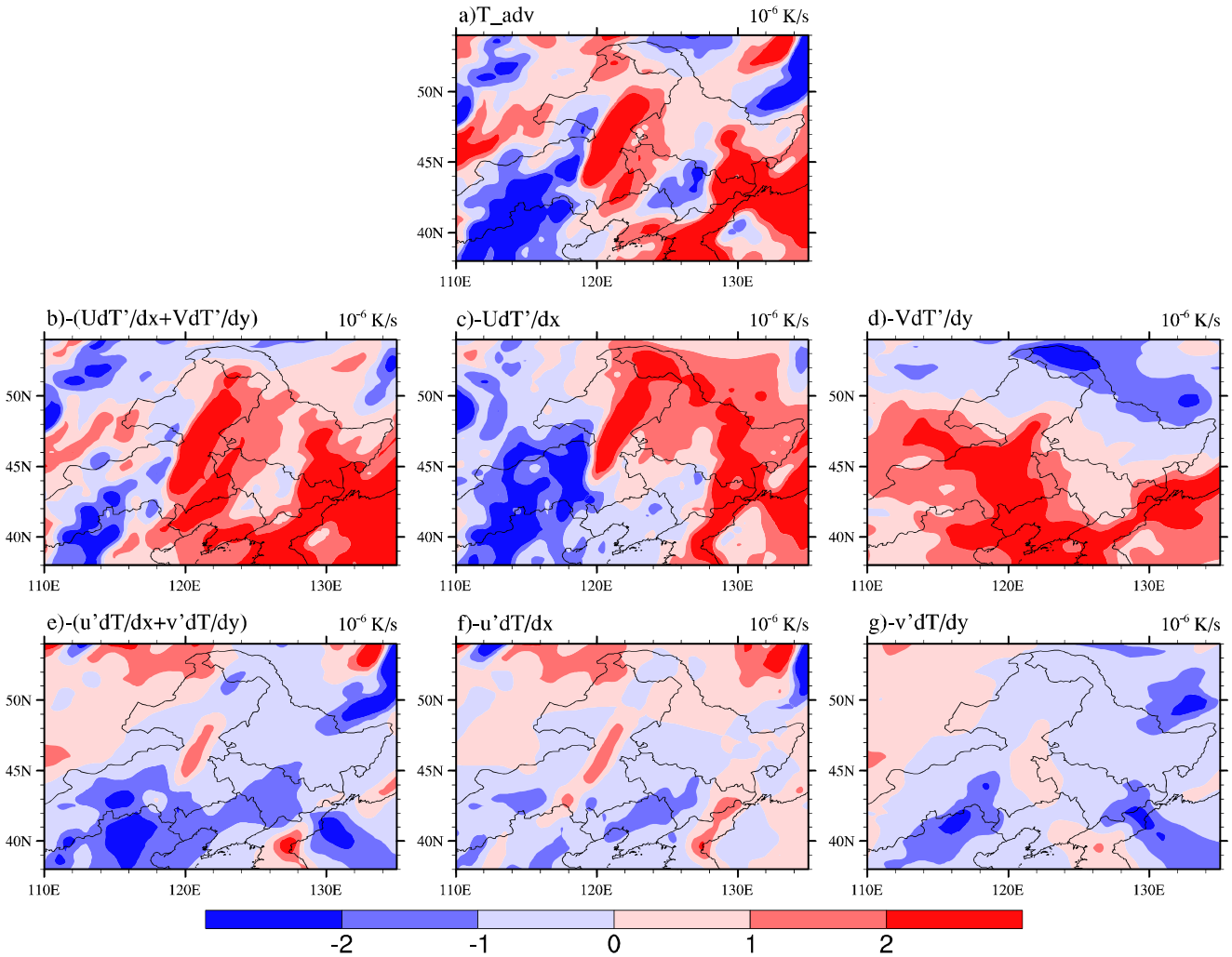

Fig. 8 Spatial distribution of the 850 hPa surface air temperature advection obtained by regression on CSAT over NEC at 850 hPa

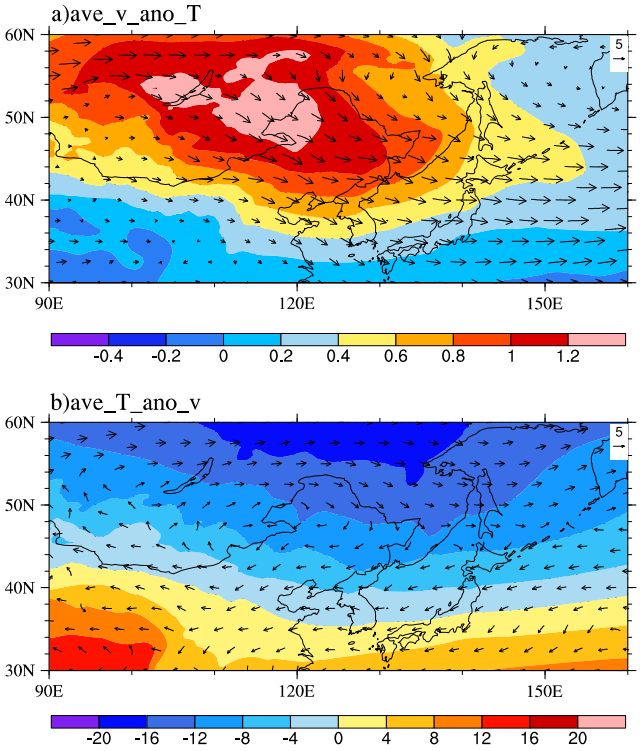

Fig. 9 **a** The climatological mean winds ($m \cdot s^{-1}$; vectors; scale at *upper-right corner*) overlaid on CSAT-related temperature anomalies. **b** The CSAT-related wind anomalies ($m \cdot s^{-1}$; vectors; scale at *upper-right corner*) overlaid on the climatological mean temperature at 850 hPa

winds overlaid on CSAT-related temperature anomalies (Fig. 9a) and the CSAT-related wind anomalies overlaid on the climatological mean temperature (Fig. 9b). The CSAT-related warm center is right located to the west of NEC; therefore, the climatological mean wind can advect the warm air eastward and southward towards the NEC, leading to warming tendency over eastern and southern portion of the NEC (Fig. 8c, d). In contrast, the anomalous anticyclone over East Asia (Figs. 6b and 9b) favors cooling tendency over NEC (Fig. 8e, f) because the CSAT-related wind anomalies blow upgradient of the climatological mean temperature field (Fig. 9b). Despite this seemingly destructive effect, this anomalous anticyclone is crucial for the formation of the anomalous warm center over Lake Baikal (Figs. 6c and 9a) because the southerly wind anomalies of the anticyclone blows downgradient of the climatological mean temperature field (Fig. 9b). Therefore, the advection effect is quite important for the variations of CSAT over NEC.

6 Linkages between the cold season climate indices and the CSAT over NEC

The circulation patterns shown in Fig. 6 are similar to those associated with the positive phase of AO (Thompson and Wallace 1998, 2000) and the positive phase of POL (Koide and Kodera 1999). The POL pattern is associated with fluctuations in the strength of the circumpolar circulation, with negative height anomalies over the polar region and positive anomalies over NEC and Mongolia in positive POL phase. It also affects large-scale atmospheric circulations and climate over Eurasia (Steinbrecht et al. 2001; Gao et al. 2016). This resemblance indicates that the CSAT over NEC could be affected by the Northern Hemispheric teleconnection patterns. In this section, we will discuss the relationship between the CSAT over NEC and the Northern Hemispheric teleconnection pattern and the involved physical mechanism.

6.1 Spatiotemporal correlation

Table 2 and Fig. 11 show the spatiotemporal correlation coefficients between the CSAT over NEC and the atmospheric climatic indices for the cold season from 1981 to 2014. The CSAT in NEC is significantly correlated with the cold season AO, POL, and NAO indices ($r = 0.62/r = 0.47$, 99% confidence level; $r = 0.33$, 95% confidence level). It indicates that when the AO, POL, and NAO are in their positive phases, the NEC tends to experience a warmer cold season (Fig. 10). The other indices shown in Table 1 are slightly correlated with the CSAT over NEC. We also compute the correlation coefficient between the SAT and the AO and POL indices in each month during the cold season (Table 3). The highest correlations occur in March and November for the AO and POL associated with the CSAT over NEC but not in winter defined as the months from December through to February. It suggests that the effect of the AO and POL on temperature are not solely from winter, which may be related to the melting of sea ice in Arctic. In March and November, the sea ice density is smaller than that in

Table 2 The correlation coefficients between the CSAT and climate indices defined in Table 1

Index name	Correlation coefficient
AO	*0.62***
NAO	*0.33***
NINO3.4	−0.01
AMO	0.19
PDO	0.22
POL	*0.47****
PNA	−0.30*
EA	−0.09
EAWR	0.29
EU	−0.30*

*90% confidence level; **95% confidence level; ***99% confidence level

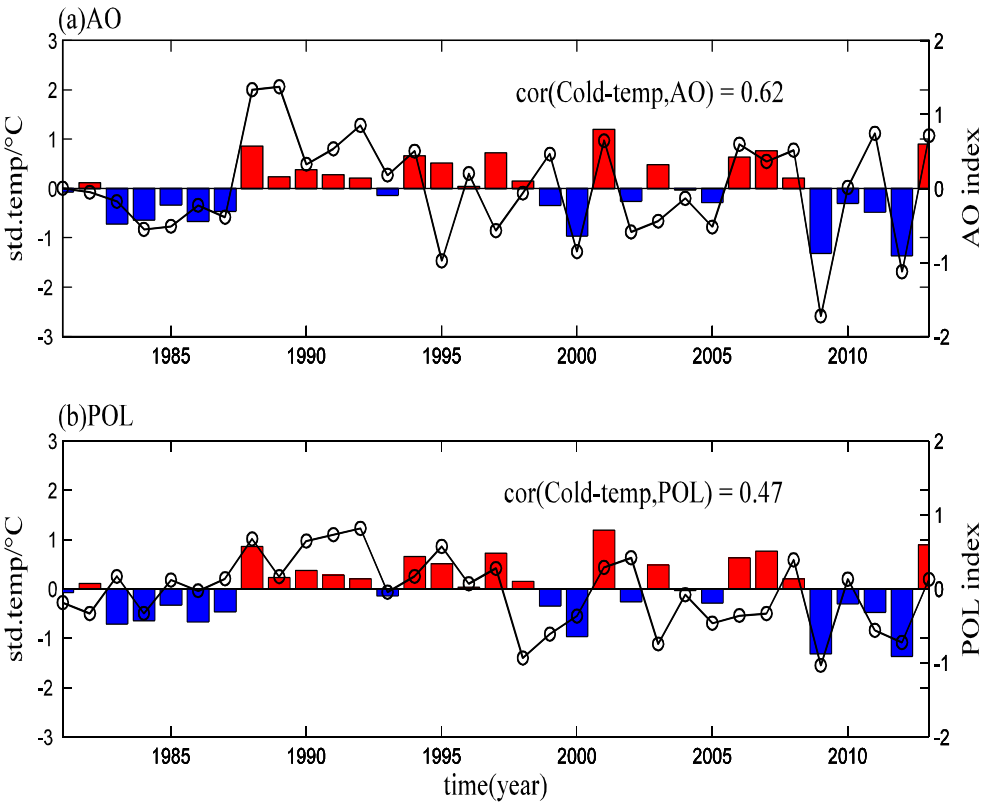

Fig. 10 The times series of the standardized CSAT (histogram) and the cold season. **a** AO index. **b** POL index (*solid line with empty circles*)

winter, which may affect the large-scale atmospheric circulation in East Asia and thereby have effect on the CSAT over NEC (Wu et al. 2010, 2015; Zhang and Wu 2011). The continuity of the influence of the AO is at its best from October to April, further illustrating the rationality of defining the cold season as the months from October to April.

Taking NEC as a whole, the CSAT variability is significantly positively correlated with the AO index. The strongest correlation, which exceeds 0.6, occurs at the junction between the north of eastern Inner Mongolia, Heilongjiang Province and near the Xilin Gol at the 99% confidence level (Fig. 11a), while the POL index is significantly positively associated with the CSAT over northern NEC (Fig. 11b), including most of Heilongjiang Province, eastern Inner Mongolia, Jilin Province and northern Hebei Province, with the maximum correlation coefficient locating at the junction between Heilongjiang Province and Russia. Compared with the AO, the POL index is more closely related with the CSAT in the north than in the south of NEC.

6.2 Associated teleconnection patterns

The EAWM is an important component of the Asian winter monsoon system. The major components of the EAWM, characterized at the surface by the cold Siberian high, the Aleutian low and northeasterly winds, a deep East Asian longwave trough in the mid-troposphere, and an upper jet at 200 hPa, are associated with the climate anomaly over East Asia (Chen et al. 2000; Jhun and Lee 2004; Chang et al. 2011; Wang and Lu 2017).

Figure 12 shows the SLP, H500, and the 850 hPa temperature anomaly (T850) as obtained by regression onto the AO index and POL index. Negative geopotential height anomalies extend from the polar region to Siberia over Eurasia and

Table 3 The correlation coefficients between the area-averaged temperature and climate indices defined Table 1 for each month during October to April

Name	Cor_10	Cor_11	Cor_12	Cor_1	Cor_2	Cor_3	Cor_4
AO	*0.30**	*0.35***	*0.46****	*0.34***	*0.45****	*0.55****	*0.19*
POL	*0.35***	*0.42***	0.24	*0.33***	0.27	0.14	*0.31**

Cor_10: the correlation coefficient between the October temperature over NEC and the October climatic index, and so on

*90% confidence level; **95% confidence level; ***99% significant level

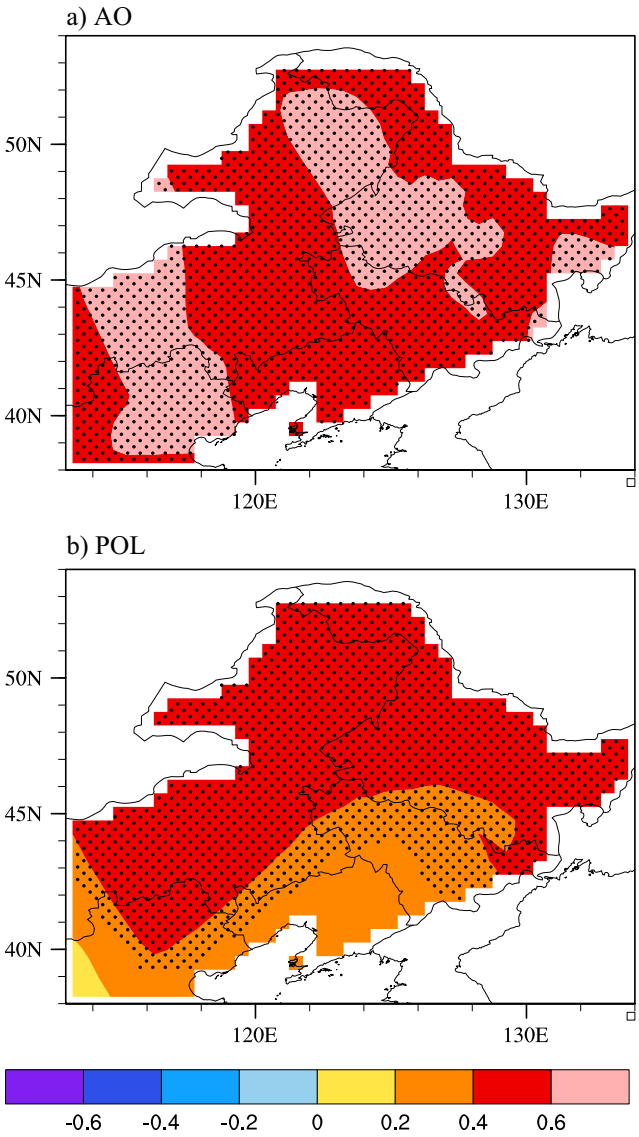

Fig. 11 The spatial distribution of the correlation coefficient between the CSAT over NEC and the **a** AO index. **b** POL index of the cold season (*dots* indicate the region where the correlations are exceeding the 95% confidence level)

positive ones over the North Atlantic, Aleutian Islands, and Lake Baikal (Fig. 12a, b). A warm center is observed over NEC at 850 hPa temperature filed (Fig. 12c). These are quite similar to those associated with the CSAT over NEC (Fig. 6). With the positive phase of the AO, an anomalous anticyclone is observed at 500 hPa over central Siberia (Fig. 12b). As discussed in Sect. 5, this anomalous anticyclone is vital for the temperature variations over the NEC via advection effect. These results suggest that the AO could realize its influences on the CSAT of NEC by the anomalous anticyclone over central Siberia.

In the positive phase of the POL, negative geopotential height anomalies are observed in the polar region and positive geopotential height anomalies are located in the high latitudes of East Asia (Fig. 12d, e). These are similar to the atmospheric circulation patterns associated with the AO, but the intensity of the influence of the POL on the CSAT over NEC is weaker than that of the AO (Fig. 11). Compared with the positive AO, the positive SLP anomaly near the Aleutian Islands becomes insignificant (Fig. 12d), increasing the East Asia–North Pacific sea–land pressure difference, strengthening the intensity of the EAWM. An increase meridional circulation weakens zonal westerly wind at 850 hPa. And the position of the zero geopotential height anomaly line in the East Asia coast northward shifts from the middle and lower of the Yangtze River to the North China at 500 hPa (Fig. 12b, e). It is contributed to enhance the East Asian major trough and favored by a stronger northerly wind over NEC. Therefore, the cold air moves southward and affecting the climate in East Asia.

As abovementioned, the AO and POL have a close relationship with the CSAT over NEC and their circulations are similar, but there are some differences in polar at 500 hPa, associated with the polar vortex (Fig. 12b, e). We compute the correlation of AO and polar vortex strength index (Table 4). Note that the position of polar vortex data is obtained from the 74 circulation parameters of the National Climate Center, including I (60E–150E), II (150E–120W), III (120W–30W), IV (30W–60E), and V (0–360). There are remarkable positive correlations between AO index and III, IV, and V polar vortex strength indices, while the negative correlation with I and II polar vortices implies that the polar vortex in eastern hemisphere shrinks in the Asia Pacific sector. This feature is shown explicitly in Fig. 12b. Namely, in the positive AO phase, the negative geopotential height anomaly center in 500 hPa towards the western hemisphere, located in 10–60°W over the north polar (Fig. 12b), strengthens III, IV, and V polar vortices.

The POL index is significantly correlated with I, III, and V polar vortex strength indices. Compared with AO index, the correlation between the POL index and the I polar vortex strength index is significant, indicating that the polar vortex in eastern hemisphere expands in East Asian. These results are similar to Fig. 12e. Namely, in positive POL phase, there are two negative centers, one in the 60°–180° E over eastern hemisphere and the other in 30°–90° W over the western hemisphere, reinforcing I, III, and V polar vortices.

Different circulation patterns are corresponding to different changes in climate. In the positive AO phase, the center of the polar vortex is located near Greenland in the western hemisphere and the zonal circulation dominates over the whole East Asian coast (Fig. 12b), so the cold air from high latitudes only has a slight influence on

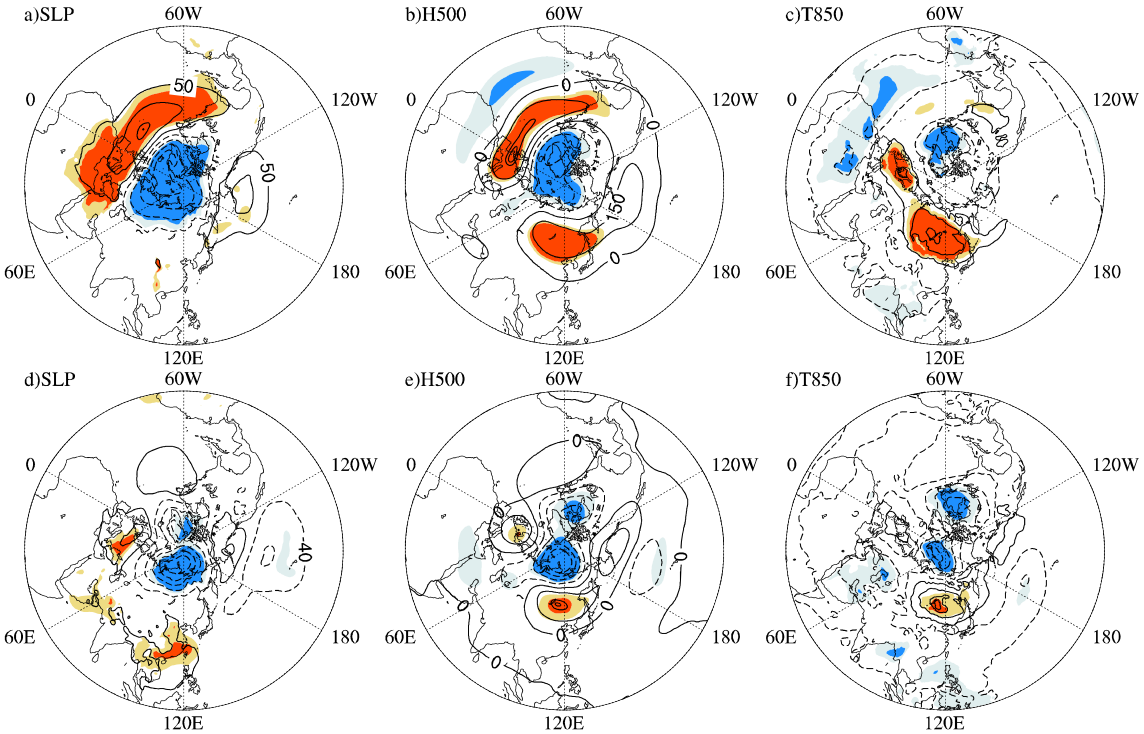

Fig. 12 As in Fig. 6, but for the cold season AO index in **a**, **b**, **c** and POL index in **d**, **e**, **f** (*light and dark shadings* indicate the 99 and 99.9% confidence levels based on a two-sided Student's *t* test, respectively. The contour intervals are 90 hPa, 150gpm, and 0.6 °C at SLP, H500, and T850, respectively)

the CSAT over NEC and the whole northeast Asia is warmer than normal (Fig. 12c). When the POL is in a positive phase, the polar vortex splits into two centers, one situates near Novaya Zemlya in the eastern hemisphere, with a stronger central intensity than that of the AO. Simultaneously, the meridional circulation behind the 500 hPa East Asian major trough strengthens (Fig. 12e), indicating that the cold air from high latitudes can flow southward as a result of the northerly wind behind the 500 hPa East Asian major trough. The East Asian region is therefore vulnerable to the effects of cold air from high latitudes. The magnitude of warming of the CSAT over East Asia is weaker than that of AO, even the warming of the northern over East Asian is not significant (Fig. 12f).

Table 4 The correlation coefficient of AO and POL index and polar vortex strength index

Name	I	II	III	IV	V
AO	−0.26	−0.15	0.63**	0.63**	0.44*
POL	0.39*	−0.14	0.50**	0.26	0.42*

Noted that I (60E–150E), II (150E–120W), III (120W–30W), IV (30W–60E), and V (0–360) are polar vortices

*95% confidence level; **99% significant level

7 Discussion and conclusions

In previous studies of the NEC climate, winter is usually defined as from December through to February. However, the cold period can last for much longer than 3 months over NEC. The monthly mean SAT values for NEC from October through to April for the period 1981–2014 are all less than 5 °C. We therefore define the cold season as the months from October through to April and investigate the variability of the CSAT over NEC and its linkage with large-scale atmospheric circulation patterns. The spatiotemporal variability of the CSAT over NEC is examined by EOF analysis. The first EOF mode explains 92.2% of the total variance, and is characterized by a monopole structure with a homogeneous temperature anomaly covering the whole NEC. The second EOF mode, explaining 4.5% of the total variance, exhibits a north–south seesaw pattern.

We also examine the relationships between the CSAT over NEC and the large-scale atmospheric circulation patterns. The CSAT over NEC is closely linked to the AO/POL indices (r = 0.62/0.47, 99% confidence level). The positive AO/POL phase tends to result in an anomalous anticyclone is observed at 500 hPa over central Siberia, which favors more clear skies and downward air streams, thus increasing the CSAT by enhancing the downward solar radiation and warming up by sinking. These results suggest that the AO/POL could realize its influences on the

CSAT of NEC by the anomalous anticyclone over central Siberia.

We further analyze the influences of radiation and temperature advection on CSAT in NEC. Results show that the anomalous anticyclone over the NEC favors clear sky. The increase of net downward solar radiation has a warming effect for the ground despite the outgoing long wave tends to cool the ground. The warmed ground can warm the surface atmosphere via upward sensible heat flux, thereby contributing constructively to the warm CSAT anomalies. On the other hand, the advection effect is quite important for the variations of CSAT over NEC. The anomalous anticyclone over NEC would favor warm advection over central Siberia via advection of climatological temperature by anomalous winds, resulting in an anomalous warm center over central Siberia. The climatological mean wind will thereby advect this anomalous warm anomaly towards the NEC, leading to warming over the NEC.

The atmospheric circulation patterns' anomalies over NEC induced by the POL are similar to those induced by the AO, but there are some differences. In positive AO phase, the East Asia–North Pacific land–sea pressure difference, the 500 hPa East Asian major trough, and the northerly wind over NEC are weaker than that in POL phase. Moreover, polar vortex in the eastern hemisphere and in the northern hemisphere is weaker. These results suggest an increase in the CSAT over the whole of northeast Asia during the cold season with a positive AO, whereas in the positive POL phase, one polar vortex in eastern hemisphere, this means that the East Asia was affected by the cold air from high attitude, and this tends to result in the degree of warming of the CSAT over East Asia in the cold season to be reduced.

In addition to the monopole structure for the CSAT over NEC, the variabilities in the CSATs in the south and north of NEC are obviously different, indicating that the variability of the CSAT over NEC is not only affected by large-scale atmospheric circulation patterns but also associated with local climatic conditions, such as the snow cover, soil humidity, soil temperature, and Arctic sea ice (Groisman et al. 1994; Yang and Wu, 2013; Wu et al. 2013).

The relationships between the large-scale atmospheric circulation patterns and the CSAT over NEC are investigated. These patterns can also jointly influence the regional climate. For example, Wang et al. (2008) demonstrated that the relationship between the El Niño Southern Oscillation and the EAWM is different between the two phases of the Pacific Decadal Oscillation. These studies showed that the climate anomalies in East Asia are significantly associated with the combined effects of the AO and the El Niño Southern Oscillation rather than only one of these circulations (Cheung et al. 2012; Chen et al. 2013b). Previous researches have indicated that the sea surface temperature and land surface conditions are important in determining the East Asian climate (Annamalai et al. 2005; Zhang and Wu 2014) and may also contribute to the variability of the CSAT over NEC. The underlying physical processes explaining the linkages to large-scale circulation patterns should be further clarified using process-based approaches.

Acknowledgments We thank the two anonymous reviewers for their constructive suggestions that improve the quality of the manuscript. The CRU TS4.00 data is available at https://crudata.uea.ac.uk/cru/data/hrg/. The ERA-Interim data is available at http://apps.ecmwf.int/datasets/. The climate indices are stored at http://www.esrl.noaa.gov/psd/data/climateindices/list/. This work is supported by the National Basic Research Program of China (2012CB955604) and the National Natural Science Foundation of China (41275089 and 41305071). Jingyong Zhang is also supported by the Jiangsu Collaborative Innovation Center for Climate Change.

References

Alessio S, Taricco C, Rubinetti S, Vivaldo G, Mancuso S (2014) Temperature and precipitation in Northeast China during the last 150 years: relationship to large-scale climatic variability. Ann Geophys 32(7):749–760. doi:10.5194/angeo-32-749-2014

Annamalai H, Liu P, Xie SP (2005) Southwest Indian Ocean SST variability its local effect and remote influence on Asian monsoons. J Clim 18(20):4150–4167. doi:10.1175/JCLI3533.1

Chang C-P, Lu M-M, Wang B (2011) The East Asian winter monsoon. The Global Monsoon System: research and forecast. In: Chang C-P et al (eds) World scientific series on Asia-Pacific weather and climate, vol. 5. World Scientific, Hackensack, pp 99–109

Chen W, Graf H-F, Huang RH (2000) The interannual variability of East Asian winter monsoon and its relation to the summer monsoon. Adv Atmos Sci 17:46–60. doi:10.1007/s00376-000-0042-5

Chen W, Yang S, Huang RH (2005) Relationship between stationary planetary wave activity and the East Asian winter monsoon. J Geophys Res 110:D14110. doi:10.1029/2004JD005669

Chen W, Wei K, Wang L, Zhou Q (2013a) Climate variability and mechanisms of the East Asian winter monsoon and the impact from the stratosphere. Chin J Atmos Sci 37(2):425–438. doi:10.3878/j.issn.1006-9895.2012.12309

Chen W, Lan XQ, Wang L, Ma Y (2013b) The combined effects of the ENSO and the Arctic Oscillation on the winter climate anomalies in East Asia. Chin Sci Bull 58(12):1355–1362. doi:10.1007/s11434-012-5654-5

Cheung HN, Zhou W, Mok HY, Wu MC (2012) Relationship between Ural–Siberian blocking and the East Asian winter monsoon in relation to the Arctic Oscillation and the El Niño–Southern Oscillation. J Clim 25(12):4242–4256. doi:10.1175/JCLI-D-11-00225.1

Dee DP, Uppala SM, Simmons AJ, Berrisford P, Poli P, Kobayashi S, Andrae U, Balmaseda MA, Balsamo G, Bauer P, Bechtold P, Beljaars ACM, van de Berg L, Bidlot L, Bormann JN, Delsol C, Dragani R, Fuentes M, Geer AJ, Haimberger L, Healy SB, Hersbach H, Hólm EV, Isaksen L, Kåohler P, Köhler M, Matricardi M, AP MN, Monge-Sanz BM, Morcrette J-J, Park B-K, Peubey C, de Rosnay P, Tavolato C, Thépaut J-N, Vitart F (2011) The ERA-Interim reanalysis: configuration and performance of the data assimilation system. Q J R Meteorol Soc 137(656):553–597. doi:10.1002/qj.828

Ding Y, Krishnamurti TN (1987) Heat budget of the Siberian High and the winter monsoon. Mon Weather Rev 115:2428–2449. doi:10.1175/1520-0493(1987)115<2428:HBOTSH>2.0.CO;2

Ding YH, Liu YJ, Liang SJ, Ma XQ, Zhang YX, Si D, Liang P, Song YF, Zhang J (2014) Interdecadal variability of the East Asian winter monsoon and its possible links to global climate change. J Meteorol Res 28(10):693–713. doi:10.1007/s13351-014-4046-y

Gao T, Yu JY, Paek H (2016) Impacts of four northern-hemisphere teleconnection patterns on atmospheric circulations over Eurasia and the Pacific. Theor Appl Climatol 1–17. doi:10.1007/s00704-016-1801-2

Gong DY (2000) Large-scale atmospheric circulation patterns and its influence on winter temperature in the Northern Hemisphere (in Chinese). Earth Sci Front 7(B08):203–208

Gong DY, Wang SW, Zhu JH (2001) East Asian winter monsoon and Arctic Oscillation. Geophys Res Lett 28(10):2073–2076. doi:10.1029/2000GL012311

Graversen RG, Kapsch M, Mauritzen T, Tjernström M (2012) Arctic temperature amplification and sea-ice melt. EGU General Assembly Conference. EGU General Assembly Conference Abstracts, 14(3):11066

Groisman PY, Karl TR, Knight RW, Stenchikov LG (1994) Changes of snow cover, temperature, and radiative heat balance over the Northern Hemisphere. J Clim 7(11):1633–1656. doi:10.1175/1520-0442(1994)007<1633:COSCTA>2.0.CO;2

Harris I, Jones PD, Osborn TJ, Lister DH (2014) Updated high-resolution grids of monthly climatic observations—the CRU TS3.10 dataset. Int J Climatol 34(3):623–642. doi:10.1002/joc.3711

Hong CC, Hsu HH, Chia HH, Wu CY (2008) Decadal relationship between the North Atlantic Oscillation and cold surge frequency in Taiwan. Geophys Res Lett 35(24):745–750. doi:10.1029/2008gl034766

Hu XL, Liu XF (2005) Decadal relationship between winter air temperature in Northeast China and Arctic Oscillations (in Chinese). J Nanjing Inst Meteorol 28(5):640–648

Hu CD, Yang S, Wu QG (2015) An optimal index for measuring the effect of East Asian winter monsoon on China winter temperature. Clim Dyns 45(9–10):2571–2589. doi:10.1007/s00382-015-2493-5

Huang RH, Chen JL, Wang L, Lin ZD (2012) Characteristics, processes and causes of the spatio-temporal variabilities of the East Asian monsoon system. Adv Atmos Sci 29(5):910–942. doi:10.1007/s00376-012-2015-x

Jhun JG, Lee EJ (2004) A new East Asian winter monsoon index and associated characteristics of the winter monsoon. J Clim 17(4):711–726. doi:10.1175/1520(2004)017<0711:ANEAWM>2.0.CO;2

Kanamitsu M, Ebisuzaki W, Woollen J, Yang SK, Hnilo J, Fiorino M, Potter G (2002) NCEP–DOE AMIP-II reanalysis (R-2). Bull Am Meteorol Soc 83(11):1631–1643. doi:10.1175/BAMS-83-11-1631

Kang LH, Chen W, Wei K (2006) The interdecadal variation of winter temperature in China and its relation to the anomalies in atmospheric general circulation (in Chinese). Clim Environ Res 11(3):330–339. doi:10.3878/j.issn.1006-9585.2006.03.09

Kang LH, Chen W, Wang L, Chen LJ (2009) Interannual variations of winter temperature in China and their relationship with the atmospheric circulation and sea surface temperature (in Chinese). Clim Environ Res 14(1):45–53. doi:10.3878/j.issn.1006-9585.2009.01.05

Koide H, Kodera K (1999) A SVD analysis between the winter NH 500-hPa height and surface temperature fields. J Meteorol Soc Jpn 77(1):47–61. doi:10.2151/jmsj1965.77.1_47

Lan X, Chen W (2013) Strong cold weather event over Eurasia during the winter of 2011/2012 and a downward Arctic Oscillation signal from the stratosphere (in Chinese). Chin J Atmos Sci 37(4):863–872. doi:10.3878/j.issn.1006-9895. 2012.12061

Li JP, Wang JXL (2003a) A modified zonal index and its physical sense. Geophys Res Lett 30(12):1632. doi:10.1029/2003GL017441

Li JP, Wang JXL (2003b) A new North Atlantic Oscillation index and its variability. Adv Atmos Sci 20(5):661–676. doi:10.1007/BF02915394

Li YQ, Yang S (2010) A dynamical index for the East Asian winter monsoon. Notes Corresp 23(15):4255–4262. doi:10.1175/2010JCLI3375.1

Lu CH, Ding YH (2015) Analysis of isentropic potential vorticities for the relationship between stratospheric anomalies and the cooling process in China (in Chinese). Sci Bull 60:726–738. doi:10.1007/s11434-015-0757-4

Steinbrecht W, Claude H, Köhler U, Winkler P (2001) Interannual changes of total ozone and Northern Hemisphere circulation patterns. Geophys Res Lett 28(7):1191–1194. doi:10.1029/1999gl011173

Thompson DWJ, Wallace JM (1998) The Arctic oscillation signature in the wintertime geopotential height and temperature fields. Geophys Res Lett 25(9):1297–1300. doi:10.1029/98gl00950

Thompson DWJ, Wallace JM (2000) Annular modes in the extratropical circulation—part I: month-to-month variability. J Clim 13(5):1000–1016. doi:10.1175/1520-0442(2000)013<1000: AMITEC>2.0.CO;2

von Storch H, Zwiers FW (1999) Statistical analysis in climate research. Cambridge Univ Press, Cambridge, pp 293–299

Wang L, Chen W (2010) Downward Arctic Oscillation signal associated with moderate weak stratospheric polar vortex and the cold December 2009. Geophys Res Lett 37(9):90–98. doi:10.1029/2010gl042659

Wang L, Chen W (2014) The East Asian winter monsoon: re-amplification in the mid-2000s. Chi Sci Bull 9(4):430–436. doi:10.1007/s11434-013-0029-0

Wang L, Lu MM (2017) The East Asian winter monsoon. In: Chang C-P, Kuo H-C, Lau N-C, Johnson RH, Wang B, Wheeler M (eds) The Global Monsoon System: research and forecast, 3rd Edition. 51–61, doi:10.1142/9789813200913_0005

Wang L, Chen W, Huang RH (2008) Interdecadal modulation of PDO on the impact of ENSO on the east Asian winter monsoon. Geophys Res Lett 35:L20702. doi:10.1029/2008gl035287

Wang L, Chen W, Fong SK (2011) The seasonal March of the North Pacific Oscillation and its association with the interannual variations of China's climate in boreal winter and spring (in Chinese). Chin J Atmos Sci 21(21):53–68

Wang L, Huang RH, Gu L, Chen W, Kang LH (2009) Interdecadal variations of the East Asian winter monsoon and their association with quasi-stationary planetary wave activity. J Clim 22:4860–4872. doi:10.1175/2009JCLI2973.1

Wu BY, Huang RH (1999) Effects of the extremes in the North Atlantic Oscillation on East Asia winter monsoon (in Chinese). Chin J Atmos Sci 23(6):641–651. doi:10.3878/j.issn.1006-9895.1999.06.01

Wu BY, Wang J (2002) Winter Arctic Oscillation, Siberian High and East Asian winter monsoon. Geophys Res Lett 29(19):1–4. doi:10.1029/2002gl015373

Wu ZW, Li J, Wang B, Liu X (2009) Can the Southern Hemisphere annular mode affect China winter monsoon? J Geophys Res 114:D11107. doi:10.1029/2008JD011501

Wu Z, Li J, Jiang Z, He J (2010) Predictable climate dynamics of abnormal East Asian winter monsoon: once-in-a-century snowstorms in 2007/2008 winter. Clim Dyn 37:1661–1669. doi:10.1007/s00382-010-0938-4

Wu BY, Handorf D, Dethloff K, Hu AX (2013) Winter weather patterns over northern Eurasia and Arctic Sea ice loss. Mon Weather Rev 141(11):3786–3800. doi:10.1175/MWR-D-13-00046.1

Wu BY, Su JZ, D'Arrigo R (2015) Patterns of Asian winter climate variability and links to Arctic sea ice. J Clim 28:150715142453002. doi:10.1175/JCLI-D-14-00274.1

Yang LN, Wu BY (2013) Interdecadal variations of the East Asian winter surface air temperature and possible causes. Sci Bull 58(32):3969–3977. doi:10.1007/s11434-013-5911-2

Yu ZY, Fan GZ, Hua W, Zhou DW, Lan X, Liu YX (2010) Variation characteristics of season start dates over China under the global warming (in Chinese). Clim Environ Res 15(1):73–82

Zhang BK (1934) The duration of four seasons in China (in Chinese). Acta Geograph Sin 1(1):29–74. doi:10.11821/xb193401002

Zhang JC, Lin GZ (1985) The climate in China (in Chinese). Shanghai Scientific and Technical Publishers, Shanghai

Zhang RN, Wu BY (2011) The northern hemisphere atmospheric response to spring Arctic sea ice anomalies in CAM3.0 model (in Chinese). Chin J Atmos Sci 35(35):847–862

Zhang JY, Wu LY (2014) Impacts of land-atmosphere interactions on climate over East Asia (in Chinese). China Meteorological Press, Beijing

Zhang Y, Sperber KR, Boyle JS (1997) Climatology and interannual variation of the East Asian winter monsoon results from the 1979–95 NCEP/NCAR reanalysis. Mon Weather Rev 125(10):2604–2619. doi:10.1175/1520-0493(1997) 125<2605:CAIVOT>2.0.CO;2